RSC Advances

PAPER

View Article Online
View Journal | View Issue



Cite this: *RSC Adv.*, 2020, **10**, 10703

# Competitive adsorption of naphthalene and phenanthrene on walnut shell based activated carbon and the verification *via* theoretical calculation†

Zhansheng Wu, *[ac] Zhonghai Sun,[b] Pengyun Liu,[c] Qing Li,[a] Renpeng Yang[a] and Xia Yang[a]

Walnut shell based activated carbon (WAC) was prepared *via* microwave-assisted KOH activation. The adsorption behaviors towards naphthalene (NAP) and phenanthrene (PHE) over WAC were studied, both in single- and binary-compound systems. Characterization results reveal the excellent microporous structure of WAC, with a micropore specific surface area of 438.5 $m^2$ $g^{-1}$. The functional groups of walnut shell precursor surface were activated through microwave irradiation. In both systems, the pseudo-second-order model can better describe the adsorption kinetic data of PAHs over WAC at all experimental conditions. Mass transfer mechanism analysis shows that film diffusion was the rate-limiting step during the adsorption process. The adsorption amount of PAHs on WAC decreased as pH values increased, and the equilibrium data can be fitted by the Freundlich isotherm model well. In binary-component systems, the presence of PHE prominently restrained the adsorption towards NAP, and the Sheindorf–Rebhun–Sheintuch (SRS) model can fully fit the adsorption equilibrium experimental values of PAHs over WAC. In addition, the preferential adsorption behavior of PHE over WAC also was confirmed by theoretical calculations. The π–π complex between the active sites on the WAC surface and π-electrons of benzene rings from PAHs may play a major role in competitive adsorption. These results indicated that WAC was a potentially low-cost adsorbent for PAH elimination.

Received 13th November 2019
Accepted 6th March 2020

DOI: 10.1039/c9ra09447d

rsc.li/rsc-advances



## 1. Introduction

Polycyclic aromatic hydrocarbons (PAHs) with several aromatic rings (≥2), commonly are derived from inadequate combustion of raw materials in coal and petrochemical industries, automotive exhaust emission and leakage of oil products. Due to their high toxicity and stability, PAHs are confirmed to be primary pollutants according to the US Environmental Protection Agency (EPA).[1–3] Due to the low biodegradability, weak ionization capacity, low water-solubility and vaporization pressure, PAHs are exceedingly resistant to natural degradation processes and have been present in the environment for a long time. Furthermore, because of accumulation in living tissues, PAHs have caused various adverse effects and disorders for human beings,[3–5] and urgently need to be removed from water environment.

To date, many different techniques such as adsorption, flocculation, coagulation, membrane filtration, solvent extraction, and biological treatment have been employed to remove PAHs from aqueous solution-solid systems.[3–5] Among the various treatments, adsorption based on several types of porous materials, such as activated carbon (AC), activated alumina, ion exchange media, and iron-based media, has been regarded as a promising green technology due to its simple operation, remarkable economic applicability, low-energy demand, and environmental friendliness.[6–8] Actually, the types of adsorbent are vital for the adsorption performances towards specific contaminants. Generally, AC is considered to be a good adsorbent owing to the developed porosity, large surface area and high adsorption capacity.[7–9] Recently, due to the low-cost and wide availability, a wide variety of biomass resources have been deployed as precursors to achieve target AC materials.[9–11] As reported, Cabal *et al.*[12] prepared AC from bean pods to remove naphthalene (NAP) from solution *via* physical adsorption. In addition, waste banana peel was adopted by Gupta *et al.*[13] to synthesize AC as an efficient and inexpensive adsorbent to eliminate PAHs from aqueous system.

[a]*School of Environmental and Chemical Engineering, Xi'an Polytechnic University, Xi'an 710048, P. R. China. E-mail: wuzhans@xpu.edu.cn; Fax: +86 02962779281; Tel: +86 02962779279*

[b]*Department of Environmental Operation Technology, Muyuan Foods Co. Ltd., Nanyang 473000, P. R. China*

[c]*School of Chemistry and Chemical Engineering, Shihezi University, Shihezi 832003, China*

† Electronic supplementary information (ESI) available. See DOI: 10.1039/c9ra09447d

Walnut shell (WNS), one of the most common agricultural by-product, has a huge quantity in China every year.[14] As a natural raw material, which is mainly composed of lignin and polysaccharides (such as hemicellulose and cellulose), it has been widely studied. Zheng *et al.*[15] prepared high-performance AC derived from WNS by heating precursors in a tube furnace to remove phenanthrene (PHE) from water. Another WNS-based AC with high specific surface area was reported by Teixeira *et al.*[16] and was synthesized by the method of conventional heating through a vertical furnace. Compared with traditional heating methods, microwave heating can directly provide energy to carbon skeleton at molecular level and save energy by reducing the reaction time.[17,18] As Ao *et al.* pointed out, microwave heating could avoid the disadvantageous factors of traditional heating methods *i.e.* the outside to inside-heat transfer mode, which will lead to the inhomogeneous heat of WNS materials and further hinder the diffusion of volatile substances and leave ash in the pore, reduce the carbon production and give poor performance of activated carbon.[19] Therefore, as an energy-efficient process, microwave-assisted irradiation is undoubtedly an alternative and novel heating method to convert biomass into AC. However, few researchers have focused on the preparation of the WNS-based AC (WAC) through microwave-assisted irradiation and their application in eliminating PAHs from aqueous solution.

Actually, many researchers mainly focus on the removal of single-component PAHs from water.[1,4,13] However, usually actual wastewater is comprised of more than one pollutant, and the adsorption behavior characteristics of mixed pollutants over adsorbent will be different from the single-component system. Thus, a study on the adsorption behavior of mixed-contaminant systems is significance and more interesting. Similarly, Hamidouche *et al.*[20] investigated the simultaneous adsorption of 2-nitrophenol and 4-nitrophenol over AC-based composite materials and confirmed the synergistic effect of these two nitrophenol compounds during the adsorption process. Ahn *et al.*[21] reported the selective adsorption of PHE in nonionic-anionic surfactant mixtures over AC and found that the selectivity for PHE adsorption is affected by the ratio of PHE to the surfactant. Zhou *et al.*[22] studied the selective removal of PAHs from surfactant solutions over organo-bentonite and revealed that the selectivity towards PAHs would be enhanced as increasing the hydrophobicity of PAHs.

However, to the best of our knowledge, the adsorption of binary-component PAHs from aqueous solution by ACs has been scarcely reported and the adsorption mechanisms have not been clearly demonstrated yet.

Herein, we evaluate the feasibility of PAHs removal by WAC which was prepared through microwave-assisted irradiation. The structure of WAC was characterized by Brunauer–Emmett–Teller (BET) analysis, Fourier transform infrared spectroscopy (FTIR), scanning electron microscopy (SEM), and point of zero charge ($pH_{PZC}$). The adsorption behaviors towards NAP and PHE in single- and binary-component systems were investigated. How the surface physicochemical properties of WAC affect the adsorption capabilities towards PAHs would be revealed. Moreover, the difference of adsorption capacities towards single-component solutions and mixtures was also investigated in equilibrium tests. Furthermore, the simultaneous/competitive adsorption mechanisms of NAP and PHE in mixtures at different mass concentration ratios ($r$ = [NAP/PHE]) were further explained by simulation calculation.

## 2. Materials and methods

### 2.1. Preparation of WAC *via* microwave-assisted irradiation

The WNS was purchased from the local market (Shihezi, China). WAC was successfully prepared from WNS by adding KOH *via* microwave irradiation. The specific preparation conditions are as follows. KOH and raw material was premixed in 2 : 1 (W/W), the compound was calcinated under 900 W for 10 min in a modified microwave oven (MM823LA6-NS, Midea, China) in $N_2$ atmosphere. Afterwards, the resultant product was washed to neutral and dried for the subsequent batch adsorption experiments.

### 2.2. Characterization of WAC

The pore structure characteristics of WAC were quantified by the analysis of nitrogen adsorption–desorption curve at −196 °C using a pore size and surface area analyzer (Micromeritics, Model ASAP 2020, USA). The surface morphology and structure was determined by JEOUL JSM-6490LV typed SEM, with a high accelerating voltage (15 kV). FTIR analysis of WAC was performed in the infrared domain range of 400–4000 $cm^{-1}$ from KBr pellets (10% solid) with a Bruker Tensor 27 spectrometer to verify surface functional groups. The $pH_{PZC}$ on the WAC surface was measured by the method of solid addition.[9]

### 2.3. Adsorption experiments

**2.3.1. Adsorption kinetics of NAP and PHE on WAC.** The adsorption kinetics of WAC towards NAP and PHE was

Table 1 The selected physicochemical properties of NAP and PHE.[18]

| PAHs | Structure | Formula | Molecular weight (g $mol^{-1}$) | Molecular dimension (nm × nm × nm) | Water solubility (ng $g^{-1}$) | log $K_{ow}$ |
|---|---|---|---|---|---|---|
| Naphthalene | 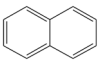 | $C_{10}H_8$ | 128.17 | 0.91 × 0.73 × 0.38 | 30 800 | 3.30 |
| Phenanthrene | 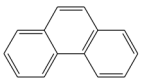 | $C_{14}H_{10}$ | 178.22 | 1.17 × 0.80 × 0.34 | 1283 | 4.57 |

 

investigated in both single- and binary-component systems. The molecular structures and properties of these compounds are summarized in Table 1. Stock solutions of NAP and PHE (50 mg $L^{-1}$) were prepared in 30% ethanol aqueous solution using ultrasound for 10 min at room temperature (25 ± 2 °C). The adsorption kinetics in single system was performed by batch experiments. A 100 mL of solution containing NAP (10 mg $L^{-1}$) or PHE (10 mg $L^{-1}$) were set pH as 7 and put in a 250 mL conical flask with stopper on a water-bathing vibrator at room temperature, and then was mixed with 0.0150 g adsorbents with immediately stirring at 170 rpm. It was start to record time now. The 20 mL solution samples were taken out by a syringe regularly after from 30 s to 160 min and filtered immediately with the membrane (0.45 μm). The concentrations of NAP and PHE of the filtrate were determined by UV-752N spectrophotometer at the maximum absorption wavelengths (219 nm for NAP and 249 nm for PHE) and the same procedure was used in binary components. The adsorption experiments were duplicated, and the average values were calculated.

The adsorption capacities of NAP and PHE at any time $t$ are expressed as $Q_t$ (mg $g^{-1}$), which was calculated by the eqn (1):

$$Q_t = \frac{(C_0 - C_t)V}{w} \quad (1)$$

where, $C_0$ (mg $L^{-1}$) and $C_t$ (mg $L^{-1}$) are the initial concentration and the concentration of PAHs at time $t$, respectively. $V$ (L) is the solution volume and $w$ (g) is the mass of the WAC.

**2.3.2. Adsorption isotherms of NAP or PHE in single-component systems.** The adsorption isotherm were carried out by changing the mass of WAC (5–100 mg) in contaminant solutions at different pH (3, 7, and 9) and mixed NAP (10 mg $L^{-1}$) or PHE (10 mg $L^{-1}$) into 100 mL of solution in conical flasks. Then, the mixture was placed on a water-bathing constant temperature shaker at 170 rpm for 40 min. The system was maintained at room temperature (25 ± 2 °C) under shaker conditions until the adsorption reached equilibrium. The pH of PAHs solution was adjusted with 0.1 M HCl and/or NaOH and then was determined with pH meter. The residual NAP/PHE concentrations in the solution were determined according to the method in 2.3.1.

**2.3.3. Adsorption isotherms of NAP or PHE in binary-component systems.** With aims to clarify the mutual influence between the two tested solutes, the experiments were performed at different concentration ratios of PAHs ($r$ = [NAP/PHE] = 1 : 0.5, 1 : 1 and 1 : 2) in aqueous solution with different pH; and the initial NAP concentration in the binary-component systems was set as 10 mg $L^{-1}$. The isotherms experiments were performed by shaking different amounts of adsorbent in the range of 5 to 100 mg. The supernatant from the mixture was obtained by filtration under the same conditions discussed above. A correction was applied for the spectrophotometric determination of residual concentrations in mixture systems by following equations:[20,23,24]

$$C_{NAP} = \frac{k_{PHE\text{-}2}d_{\lambda_{NAF}} - k_{PHE\text{-}1}d_{\lambda_{PHE}}}{k_{NAP\text{-}1}k_{PHE\text{-}2} - k_{NAP\text{-}2}k_{PHE\text{-}1}} \quad (2)$$

$$C_{PHE} = \frac{k_{NAP\text{-}1}d_{\lambda_{PHE}} - k_{NAP\text{-}2}d_{\lambda_{NAF}}}{k_{NAP\text{-}1}k_{PHE\text{-}2} - k_{NAP\text{-}2}k_{PHE\text{-}1}} \quad (3)$$

where $C_{NAP}$ and $C_{PHE}$ (mg $L^{-1}$) are the concentrations of NAP and PHE, respectively; $k_{NAP\text{-}1}$, $k_{NAP\text{-}2}$, $k_{PHE\text{-}1}$, and $k_{PHE\text{-}2}$ represent the calibration constants of NAP and PHE at their characteristic adsorption wavelength ($\lambda_{NAP}$ and $\lambda_{PHE}$); $d_{\lambda_{NAF}}$and $d_{\lambda_{PHE}}$ are the optical densities of these two wavelengths.

**2.3.4. Evaluation of model practicability.** To evaluate the validity of the selected kinetic and isotherm models in the present study, the regression of determination coefficient ($R^2$) and residual root-mean squared error (RMSE) were employed to assess the adsorption data. The RMSE equation can be expressed as follows:[23]

$$RMSE = \sqrt{1\Big/(n-1)\sum_{n=1}^{n}\left(Q_{t,exp,n} - Q_{t,cal,n}\right)^2} \quad (4)$$

where, $Q_{t,exp}$ and $Q_{t,cal}$ (mg $g^{-1}$) are the experimental adsorption capacity and predicted adsorption capacity from the model at time $t$, and $n$ is the number of observations. The highest $R^2$ and the lowest RMSE values suggest a better fitted model.

**2.3.5. Implementation of simulation.** Monte-Carlo simulations were employed to explore the interaction energies of NAP or PHE on WAC surface in several cases using the Adsorption Locator code from the Materials Studio 7.0.[25,26] And various geometric structures of WAC and NAP or PHE (WAC-1 to WAC-10) are simulated to obtain optimal and energy-minimizing contact modes during the adsorption process.

## 3. Results and discussion

### 3.1. Characterization of WAC

The curves of nitrogen adsorption–desorption, variation of pore diameter and pore volume are presented in Fig. 1. According to the International Union of Pure and Applied Chemistry (IUPAC), the current isotherm is classified as type I which suggests that the adsorption process occurred on a micropore

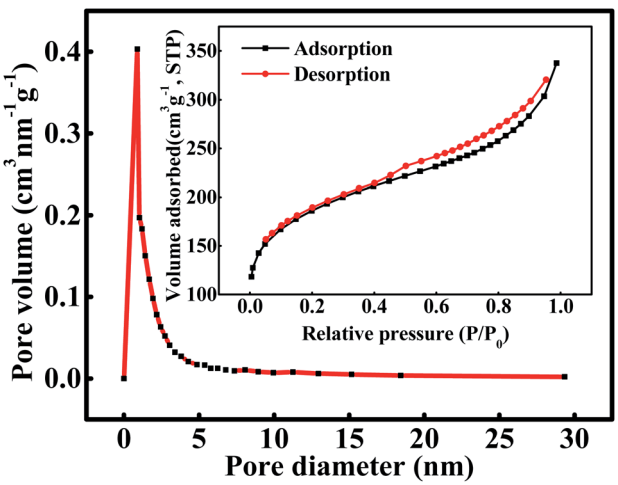


Fig. 1 The pore size distribution and nitrogen adsorption–desorption curve of WAC.

Table 2 The physical properties of prepared WAC

| Properties | $S_{BET}$ ($m^2$ $g^{-1}$) | $A_m$ ($m^2$ $g^{-1}$) | $A_e$ ($m^2$ $g^{-1}$) | $V_{mic}$ ($cm^3$ $g^{-1}$) | $V_{mes}$ ($cm^3$ $g^{-1}$) | Pore diameter (nm) | $pH_{pzc}$ |
|---|---|---|---|---|---|---|---|
| WAC | 614.24 | 438.5 | 175.77 | 0.18 | 0.21 | 0.889 | 6.78 |

(<2 nm) material. In addition, a marked hysteresis loop was observed at high relative pressures, which indicated the presence of mesoporosity. Detailed pore characteristic parameters of WAC are listed in Table 2. The specific surface area ($S_{BET}$), micropore area ($A_m$), external surface area ($A_e$), micropore volume ($V_{mic}$), and mesopore volume ($V_{mes}$) of WAC showed a significant improvement, which demonstrated that microwave irradiation can promote pore development and expansion.[11] The $A_m$ of WAC was 2.5 times of the $A_e$, which may contribute to the adsorption capacity of PAHs, because the active site of the adsorption reaction was mainly located at the microporous area.[13]

The surface morphology of WAC (Fig. 2) was examined by SEM. Indeed, the prepared WAC had a highly developed overall pore structure and rough surface with a series of uniform microporous perforation-like structures distributed over the surface, which could be mainly liable for the PAHs adsorption onto the WAC surface.

The FTIR spectrum of WAC is demonstrated in Fig. 3 to illustrate the surface functional. A wide and strong band located at 3432 $cm^{-1}$ represent the O–H stretching vibration of alcohols, phenols, and carboxylic acids from the lignin and cellulose. The twin peaks at 2976 $cm^{-1}$ and 2876 $cm^{-1}$ could be due to the anti-symmetrical stretching vibration and symmetrical stretching vibration of $-CH_3$ from the extractives in WNS.[10] The peaks detected at 1629.80 $cm^{-1}$ and 1400.92 $cm^{-1}$ correspond to C=O stretching and aromatic C=C bond or various substitution modes of the aromatic ring.[4] The peak at 1069.15 $cm^{-1}$ can be ascribed to C–O stretching of alcohols.[11] As well, the band between 500 $cm^{-1}$ and 600 $cm^{-1}$ can be assigned to the benzene derivatives.[18] These results provided robust evidence that functional groups can be activated under microwave irradiation.

### 3.2. Adsorption kinetics

The kinetic data of NAP and PHE adsorption onto WAC were described by the non-linear fitting of the pseudo-first-order, pseudo-second-order, and Elovich kinetic models,[20,27,28] respectively, which can be expressed as follows:

$$\text{The pseudo-first-order model: } Q_t = Q_e(1 - \exp^{-k_1 t}) \quad (5)$$

$$\text{The pseudo-second-order model: } Q_t = k_2 Q_e^2 t/(1 + k_2 Q_e t) \quad (6)$$

$$h = k_2 Q_e^2 \quad (7)$$

$$\text{The Elovich model: } Q_t = a + b \ln t \quad (8)$$

Where, $Q_e$ (mg $g^{-1}$) is the adsorption capacity of PAHs on sorbent at equilibrium (min); $k_1$ ($min^{-1}$) and $k_2$ (g $mg^{-1}$ $min^{-1}$) are the adsorption rate constants of the pseudo-first-order and the pseudo-second-order models; and $h$ (mg $g^{-1}$ $min^{-1}$) is the origin adsorption rate obtained from the pseudo-second-order model.

Fig. 4a shows the adsorption kinetic curves of NAP and PHE adsorption over WAC in single-component systems at 25 °C. It can be easily observed that two sorption steps appeared in the whole adsorption process. The first stage was the rapid adsorption of NAP and PHE over WAC in the initial 20 min, and the second stage continued adsorption at a slower rate until 40 min of the adsorption almost reached equilibrium and maintained a steady-state stage. This phenomenon has been reported earlier.[17,29] The calculated kinetic model parameters are listed in Table 3, it can be seen that compared with pseudo-first-order and Elovich models, the pseudo-second-order model can provide higher $R^2$, and the calculated values of $Q_e$ ($Q_{e,cal}$) are

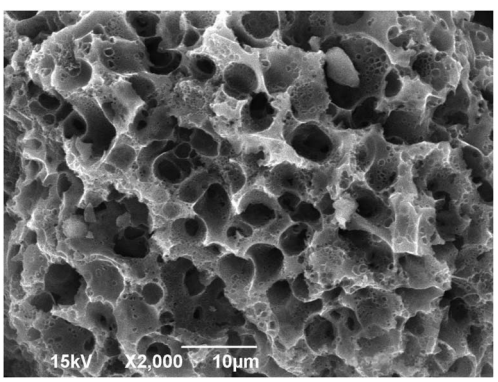


Fig. 2 The SEM of WAC.

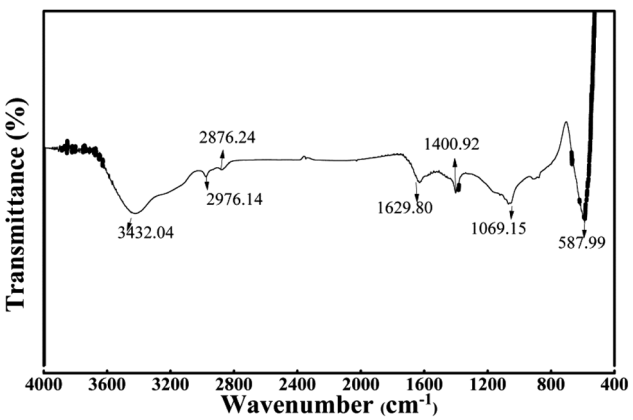


Fig. 3 The FTIR spectra of WAC.

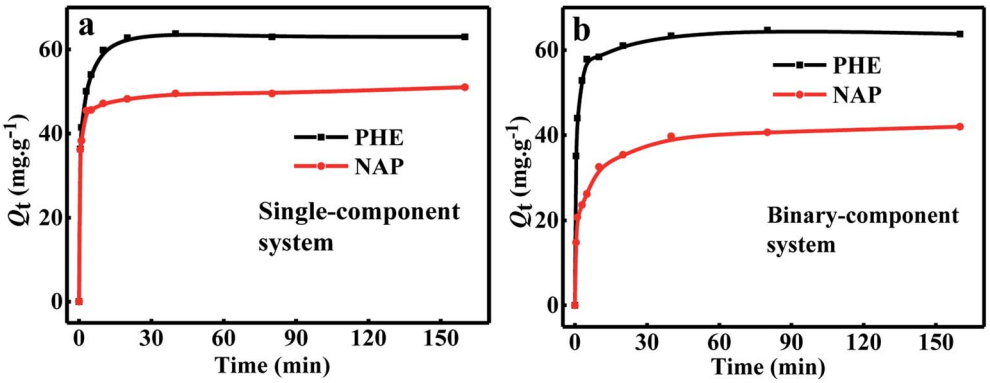


Fig. 4 The kinetic curves of NAP and PHE onto WAC in single-component (a) and binary-component (b) systems. (Conditions: $w = 0.0150$ g; [NAP] = 10 mg L$^{-1}$; [PHE] = 10 mg L$^{-1}$; shaking speed = 170 rpm.)

closer to their experimental values ($Q_{e,exp}$). Therefore, the adsorption kinetics of single-NAP and single-PHE solute was effectively described by the pseudo-second-order model suggesting that the adsorption rate of PAHs is dependent on the availability of the adsorption sites. And the adsorption process may be involved in chemisorption, including valence forces appear through electrons sharing between the hydrophobic edge sites of WAC and PAHs.[10,30] Similar results have been reported that the adsorption kinetics of PAHs on various materials was consistent with the pseudo-second-order kinetic model, such as biomass-based AC,[31] natural and chemically modified bentonite,[32] and particulate organic matters.[33]

Fig. 4b illustrates the adsorption kinetic curves in binary-component systems ([NAP] = [PHE] = 10 mg L$^{-1}$). Obviously, there was no significant change in the adsorption amount of PHE in single- and binary-component systems at equilibrium moment. However, the equilibrium adsorption amount of NAP in the binary-component system significantly reduced by 20.17% than that in the single-component system. These results indicated that the adsorption kinetics of NAP was a competitive process that is substantially affected by the presence of PHE.[20,23,24] Previous studies revealed that the same adsorbent would perform a higher adsorption capacity for PHE than NAP. Ge *et al.*[34] found that the adsorption amount of PAHs on Fe-modified AC followed the same order, and Xiao *et al.*[18] reported similar behavior during the adsorption of NAP, PHE, and pyrene over AC in solution.

According to Ahn and Diao *et al.*, the similar molecular sizes of adsorbates or when they compete for the same adsorption sites of adsorbates can lead to a competitive adsorption.[21,26] As shown in Table 1, PHE and NAP perform similar molecular dimensions and both are the strong hydrophobic compounds.

Table 3 Parameters of pseudo-first-order, pseudo-second-order and Elovich models for NAP and PHE adsorption onto WAC in the single and binary component system

| Systems | Adsorbates | $C_0$ mg L$^{-1}$ | $Q_{e,exp}$ mg g$^{-1}$ | Pseudo-first-order | Pseudo-second-order | Elovich |
|---|---|---|---|---|---|---|
| Single-component | NAP | 10 | 49.58 | $Q_{e,cal} = 47.78$<br>$k_1 = 2.361$<br>$R^2 = 0.667$<br>RMSE = 2.779 | $Q_{e,cal} = 49.12$<br>$K_2 = 0.0094$<br>$H = 22.68$<br>$R^2 = 0.992$<br>RMSE = 1.414 | $a = 40.07$<br>$b = 2.48$<br>$R^2 = 0.868$<br>RMSE = 1.749 |
| | PHE | 10 | 63.77 | $Q_{e,cal} = 59.97$<br>$k_1 = 1.432$<br>$R^2 = 0.711$<br>RMSE = 5.292 | $Q_{e,cal} = 62.96$<br>$k_2 = 0.0335$<br>$H = 132.79$<br>$R^2 = 0.956$<br>RMSE = 2.669 | $a = 43.64$<br>$b = 5.08$<br>$R^2 = 0.878$<br>RMSE = 3.441 |
| Binary-component | NAP | 10 | 39.58 | $Q_{e,cal} = 37.50$<br>$k_1 = 0.3903$<br>$R^2 = 0.650$<br>RMSE = 5.454 | $Q_{e,cal} = 39.25$<br>$K_2 = 0.0181$<br>$H = 27.88$<br>$R^2 = 0.917$<br>RMSE = 2.656 | $a = 19.36$<br>$b = 4.86$<br>$R^2 = 0.843$<br>RMSE = 3.905 |
| | PHE | 10 | 63.37 | $Q_{e,cal} = 60.00$<br>$k_1 = 1.486$<br>$R^2 = 0.773$<br>RMSE = 4.575 | $Q_{e,cal} = 62.80$<br>$k_2 = 0.0358$<br>$h = 141.89$<br>$R^2 = 0.944$<br>RMSE = 2.271 | $a = 44.13$<br>$b = 4.93$<br>$R^2 = 0.867$<br>RMSE = 3.495 |

Table 4 Single isotherm parameters evaluated by the different models for the sorption of NAP and PHE on WAC at different pH values

| | | NAP | | | PHE | | |
|---|---|---|---|---|---|---|---|
| Isotherms | Parameters | pH = 3 | pH = 7 | pH = 9 | pH = 3 | pH = 7 | pH = 9 |
| Langmuir | $K_L$ (L mg$^{-1}$) | 0.52 | 0.24 | 0.34 | 7.36 | 2.56 | 4.94 |
| | $Q_{max}$ (mg g$^{-1}$) | 118.18 | 110.28 | 74.55 | 149.62 | 117.37 | 92.03 |
| | $R^2$ | 0.983 | 0.995 | 0.972 | 0.960 | 0.955 | 0.939 |
| | RMSE | 3.34 | 3.17 | 2.62 | 9.29 | 11.13 | 7.33 |
| Freundlich | $K_F$ | 33.27 | 22.86 | 18.78 | 105.81 | 65.98 | 59.86 |
| | $n$ | 1.79 | 1.58 | 1.84 | 3.10 | 2.83 | 3.34 |
| | $R^2$ | 0.984 | 0.998 | 0.992 | 0.979 | 0.967 | 0.964 |
| | RMSE | 3.34 | 1.44 | 1.32 | 6.72 | 6.24 | 5.67 |
| Tempkin | $B$ | 22.17 | 23.11 | 16.26 | 18.81 | 12.58 | 10.97 |
| | $A$ (L mg$^{-1}$) | 6.66 | 3.15 | 3.47 | 399.37 | 260.04 | 362.44 |
| | $R^2$ | 0.983 | 0.989 | 0.995 | 0.910 | 0.718 | 0.821 |
| | RMSE | 3.44 | 3.17 | 1.12 | 13.86 | 18.85 | 12.59 |

Therefore, the differences adsorption behavior in single- and binary- component systems can be interpreted as follow. On the one hand, the pores of WAC in this study were predominately micropores (0.889 nm), and the dimensions of NAP and PHE were 0.73 and 0.80 nm, respectively. The size of WAC was compatible to PHE, hence the adsorption ability towards PHE by WAC is stronger than NAP and more difficult to desorb. While the micropore characteristic of WAC usually act as a channel for NAP to diffuse into the appropriate pore, but in fact there is few such pores. Therefore, WAC showed a certain degree of molecular sieving behavior toward PAHs.[2,9,31,35] On the other hand, PHE had more excellent hydrophobicity and more benzene rings than NAP, and WAC also has good hydrophobicity. Hence, this is indicating that PHE has significantly higher adsorptive affinity with hydrophobic groups on the surface of WAC surface, as well as more intense π–π interaction between π-electrons of PHE and benzene rings of WAC surface.[18,34,35] In summary, the inherent physicochemical advantages between PHE and WAC endow it with more competitive regardless of the type of adsorption system. So, since WAC preferential adsorption towards to PHE, this can explained that the adsorptive difference of the two PAHs in combination with $Q_e$ and $Q_{cal}$ values, of which PHE did not significantly change, while NAP declined in both components.[18,20,23]

Moreover, the higher values of $R^2$ and RMSE indicated that the adsorption kinetics process of PHE and NAP over WAC in binary-component system also fitted the pseudo-second-order model. The values of $k_2$ and $h$ for PHE were much higher than that of NAP both in the single- and binary-component systems (Table 3), which proves that the adsorption capability of WAC towards PHE is superior to NAP. As well, compared with single component system, the value of $k_2$ for PHE almost no changed in the binary-component systems, while it for NAP had an obvious increase by 48.07%, this phenomenon further confirms the above conclusion. In addition, the values of $h$ for NAP and PHE were also increased in the binary-component system than that in the single-component system. This interesting finding may be explained by the following discussion. Due to the limited active site on the WAC surface and direct completion that occurs at the same adsorption sites, the active sites would be preferentially occupied by more affinity contaminants (PHE),[9,11,23] whether in single-component or binary-component system, which led to a slight change in the adsorption rate of PHE. The remaining fewer adsorption sites did not carry out the adsorption interaction easily because on one hand, the adsorption in the PHE was not fully utilized; on the other hand, the adsorption of NAP was not carried out during the preferential adsorption of PHE. The adsorption rate of NAP in unit activity site was significantly improved, due to its high existing concentration in the solution which provided a larger driving force. These findings also proved that the adsorption of NAP and PHE may be involved in competition effects in the binary-component systems.[20] These results were different than Yuan's observations, which reported the sorption of five kinds of PAHs (NAP, PHE, fluorene, pyrene, and fluoranthene) using petroleum-coke porous carbon and found out that the competitive adsorption had insignificant roles in determining equilibrium adsorption of the mixed PAH in surfactant solution.[35]

### 3.3. Adsorption isotherms in single-component system

The Langmuir, Freundlich, and Tempkin isotherm models were introduced to evaluate the equilibrium experimental data by virtue of the method of non-linear analyses.[30] The relevant equations are as follows:

$$\text{Langmuir model: } Q_e = Q_{max}K_LC_e/(1 + K_LC_e) \quad (9)$$

$$\text{Freundlich model: } Q_e = K_FC_e^{1/n} \quad (10)$$

$$\text{Tempkin model: } Q_e = B\ln(AC_e) \quad (11)$$

where $C_e$ (mg L$^{-1}$) is the equilibrium concentration towards NAP or PHE in aqueous solution, $Q_{max}$ (mg g$^{-1}$) and $K_L$ (L mg$^{-1}$) are the Langmuir constants that are corresponding to maximum adsorption capacity and adsorption rate, respectively; $K_F$ (L mg$^{-1}$) and $1/n$ are the Freundlich coefficients that

 

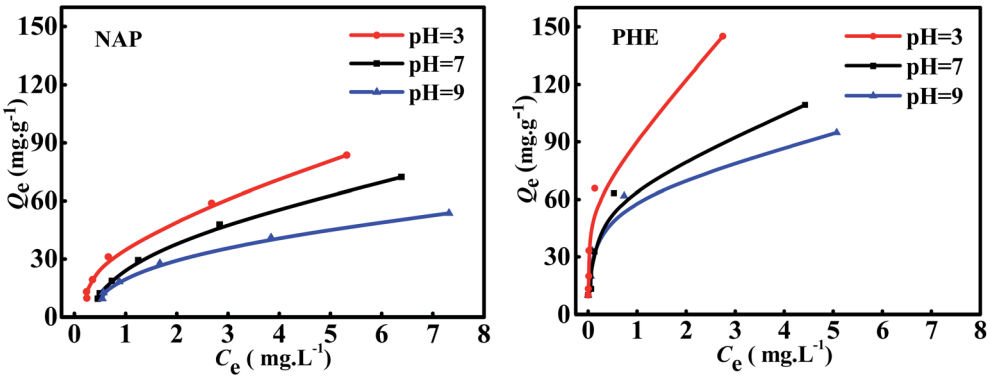


Fig. 5 Adsorption isotherms of NAP and PHE on WAC in single-component systems (conditions: [NAP] = [PHE] = 10 mg $L^{-1}$; mass of adsorbent: 5–100 mg; contact time: 40 min; shaking rate: 170 rpm).

correlated to the adsorption degree or strength and the distribution of energy in the isotherm, respectively; $A$ (L $mg^{-1}$) is the equilibrium binding constant of Tempkin, and $B$ is the Tempkin coefficient. The adsorption isotherm data were verified by $R^2$ and RMSE function values to determine the suitability of the above isotherm models.

Fig. 5 shows the adsorption isotherms of WAC for NAP and PHE under the single-component system with pH as a variable. The overall trend demonstrated that the adsorption curves of NAP were similar to those of PHE; the adsorption capacity of both NAP and PHE were reduced as pH values increased, and the $Q_{max}$ of NAP (83 mg $g^{-1}$) and PHE (145 mg $g^{-1}$) were obtained at pH = 3. This phenomenon can be interpreted as: the WAC surface was positive charge when pH < $pH_{pzc}$ (6.78), which strengthens the electrostatic attractions between WAC and NAP or PHE. While in alkaline solution (pH > $pH_{pzc}$), high $OH^-$ concentration would result in the poor positivity of WAC, and the electrostatic attraction effect between them was weakened subsequently.[20,23] In addition, the excellent adsorption capacity of WAC at low pH is also attributed to the strong electron–donor–acceptor interaction between the aromatic rings of PAHs molecule and the functional groups on the WAC surface.[9,35] Previous studies also have demonstrated that acidic solution systems can enhance the adsorption amount of NAP and PHE.[13,17]

Table 5 Competition coefficients from the SRS model

| pH | $r$ = [NAP/PHE] | $a_{NAP/PHE}$[a] | RMSE | $a_{PHE/NAP}$[a] | RMSE |
|---|---|---|---|---|---|
| pH = 3 | 1 : 0.5 | 4.13 | 6.31 | 0.24 | 1.59 |
| | 1 : 1 | 1.59 | 5.66 | 0.63 | 3.34 |
| | 1 : 2 | 1.42 | 11.73 | 0.70 | 8.17 |
| pH = 7 | 1 : 0.5 | 4.77 | 7.23 | 0.23 | 1.75 |
| | 1 : 1 | 2.95 | 7.80 | 0.34 | 3.43 |
| | 1 : 2 | 0.76 | 9.42 | 1.32 | 12.32 |
| pH = 9 | 1 : 0.5 | 5.04 | 8.91 | 0.20 | 1.94 |
| | 1 : 1 | 3.39 | 9.32 | 0.29 | 3.15 |
| | 1 : 2 | 1.34 | 12.20 | 0.75 | 9.02 |

[a] The competition coefficients: $a_{NAP/PHE} \times a_{PHE/NAP} = 1$.

The isotherm parameters obtained in NAP and PHE adsorption over WAC at different pH in single-component system for the three models are exhibited in Table 4. The $Q_{max}$ from the Langmuir isotherm model decreased when pH values increased from 3 to 9. This observation could be elucidated by this explanation that the solubility of PAHs also escalated with the increasing pH, which caused a stronger interaction of solute–solvent than that of solute-adsorbent. Furthermore, the mass transfer of NAP or PHE onto the WAC became more difficult. Compared with Tempkin and Langmuir models, the Freundlich model performed higher $R^2$ values and the lower RMSE values, which indicate that the Freundlich model are more suitable to describe the adsorption isotherm at the pH 3–9, and multi-layer adsorption possibly occurred between the PAHs molecules and WAC surface. These results demonstrated that the WAC surface may be uniformly distributed in heterogeneous moieties. The high $n$ values ($n$ > 1) from Freundlich model suggested that the NAP or PHE adsorption over WAC was favorable in the single-component system due to the formation of chemical bond between active site of the adsorbent surface and the PAHs molecules.[11,20] The values of $K_F$ for NAP and PHE increased by 77.16% and 76.76%, respectively, as the solution pH decreased from 9 to 3, which means that the adsorption was enhanced at low pH.[32] Meanwhile, the $K_F$ of PHE was always greater than that of NAP, indicating that the adsorption capacity of NAP over WAC was less than that of PHE, and this finding was consistent with the observations of the adsorption kinetics. A number of studies also demonstrated that the adsorption process of PAHs on various adsorbents were a better fit on Freundlich model compared with other isotherm models, such as petroleum coke-derived porous carbon,[35] bean pods-based AC,[12] hexadecyltrimethylammonium bromide-modified fibric peat,[36] and fatty acid-modified WNS.[4]

### 3.4. Adsorption isotherms in binary-component systems

Adsorption experiments on binary-component systems were performed by changing the value of $r$ at different pH (3, 7, and 9). To reveal the effect of $r$ on the adsorption of PAHs in binary-component system, the competition coefficients of NAP *versus* PHE ($a_{NAP/PHE}$) and PHE *versus* NAP ($a_{PHE/NAP}$) were introduced

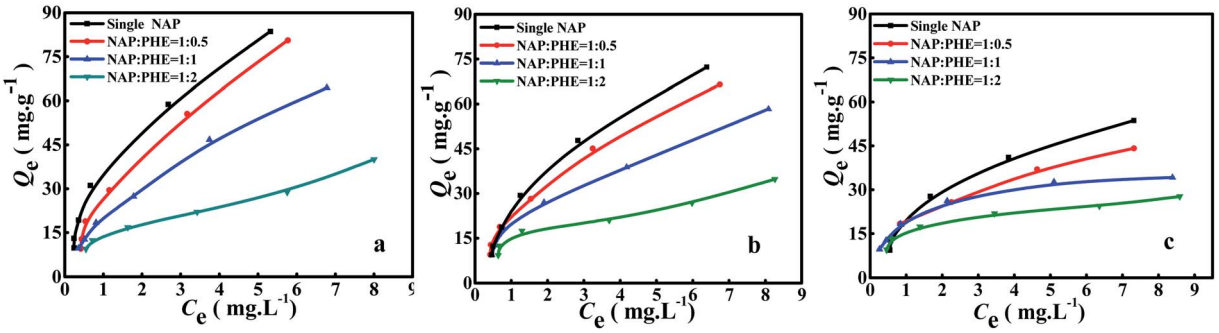


Fig. 6 Adsorption of NAP in the presence of PHE at different pH. (a) pH 3, (b) pH 7 and (c) pH 9, and at different ratios $r$ = [NAP/PHE] ($r$ = 2, 1 and 0.5).

from an extended Freundlich model established by Sheindorf–Rebhun–Sheintuch (SRS).[23] They can be defined as follows:

$$Q_{e,NAP} = K_{NAP}C_{e,NAP}(C_{e,NAP} - a_{NAP/PHE}C_{e,PHE})^{n_{NAF-1}} \quad (12)$$

$$Q_{e,PHE} = K_{PHE}C_{e,PHE}(C_{e,PHE} - a_{PHE/NAP}C_{e,NAP})^{n_{PHE-1}} \quad (13)$$

where $Q_{e,NAP}$, $C_{e,NAP}$, $Q_{e,PHE}$, and $C_{e,PHE}$ are the adsorption capacity and concentration of NAP and PHE at equilibrium, respectively; $K_{NAP}$, $K_{PHE}$, $n_{NAP}$, and $n_{PHE}$ are the Freundlich constants obtained from the single-system isotherms. The eqn (12) and (13) were based on the premise that each component complies with the Freundlich model in the single system and this evidence is confirmed in Table 4.

The calculated parametric values of $a_{NAP/PHE}$ and $a_{PHE/NAP}$ at different $r$ are summarized in Table 5. It can be found that the $a_{NAP/PHE}$ and $r$ exhibit a positive correlation at all pH values in the test condition, while $a_{PHE/NAP}$ show a opposite trend at the same $r$. These findings may be attributed to the relative content of PHE in aqueous solution increased with the reduction of $r$. As well, NAP has more surrounding PHE, thus more effective collision would occur between PHE and a certain limited active adsorption site on WAC surface. It can also be seen that the NAP adsorption decreased as the value of $r$ was lowered (Fig. 5), this may be owing to there are few remaining bare adsorption sites on WAC that are not occupied by PHE. In addition, the adsorption of PHE over WAC was higher than that of NAP at acidic solution (pH = 3) (Fig. 6 and 7). These results were consistent with the single-component isotherm-adsorption experiment.[20,23,24]

### 3.5. Preferential adsorption of NAP and PHE by WAC and its theoretical calculations

To compare with the single-component system and to further explore the competitive adsorption behavior of the active sites in binary-component system, the separation factor ($\alpha_B{}^A$) was introduced to analyze the preferential adsorption between NAP and PHE,[37] which can be described as:

$$\alpha_B{}^A = Q_{e,A}C_{e,B}/(Q_{e,B}C_{e,A}) \quad (14)$$

The parameters of the formula were obtained from equilibrium sorption data according to the adsorption isotherms in binary-component system studies. If the separation factor $\alpha_B{}^A$ is greater than unity, it means that $A$ is the preferred adsorption; otherwise, $B$ is preferentially adsorbed. The separation factor in the present case can be defined as:

$$\alpha_{NAP}^{PHE} = Q_{e,PHE}C_{e,NAP}/(Q_{e,NAP}C_{e,PHE})(PHE–NAP) \quad (15)$$

$$\alpha_{PHE}^{NAP} = Q_{e,NAP}C_{e,PHE}/(Q_{e,PHE}C_{e,NAP})(NAP–PHE) \quad (16)$$

Fig. 8 exhibits the variation of the separation factors of two substances in solutions with different pH values, where the

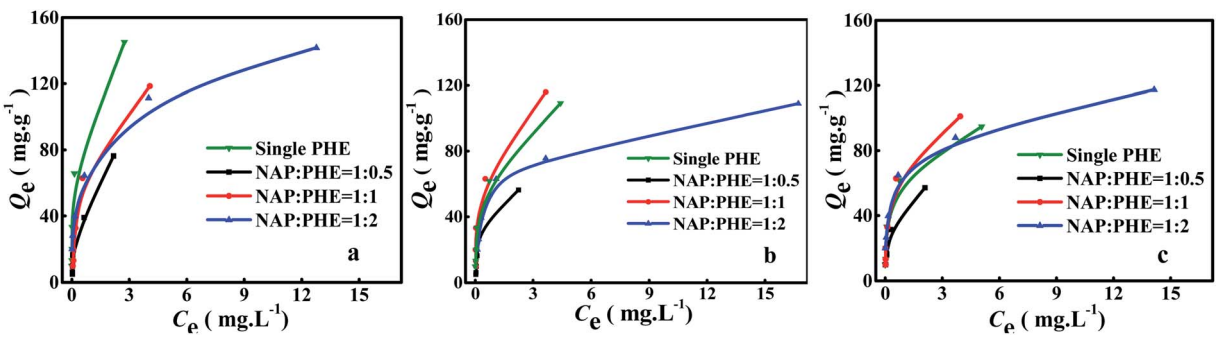


Fig. 7 Adsorption of PHE in the presence of NAP at different pH: (a) pH 3, (b) pH 7 and (c) pH 9, and at different ratios $r$ = [NAP/PHE] ($r$ = 2, 1 and 0.5).

 

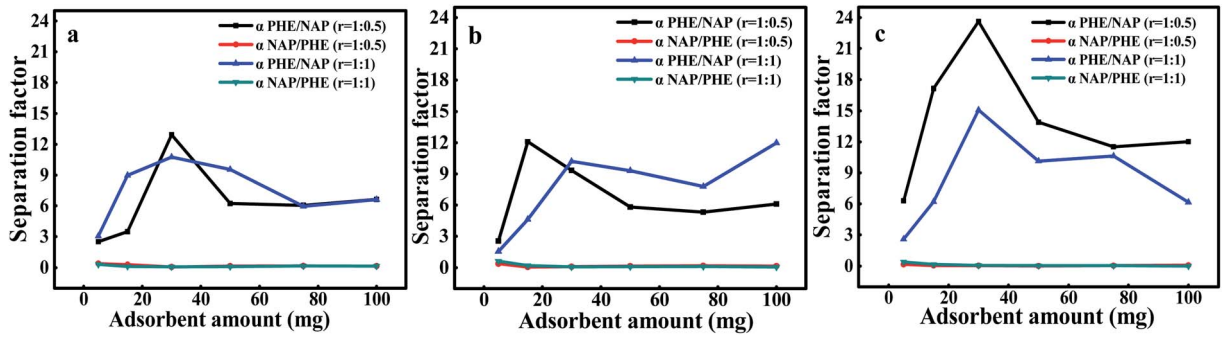


Fig. 8 The separation factors in the different proportions of components at different pH, (a) pH 3, (b) pH 7 and (c) pH 9.

separation factors are not shown as the $r$ was 1 : 2, because it was much larger than 1. Obviously, the values of separation factor for PHE-NAP were greater than unity in all cases, which indicates that PHE had greater affinity with WAC surface than NAP. In addition, the separation factors of NAP-PHE were smaller than unity in all cases, which demonstrates that PHE was preferentially adsorbed compared to NAP. This result was also consistent with the conclusion of the binary-component systems adsorption kinetics. Furthermore, the physicochemical properties of WAC and PAHs significantly affected the adsorption performance. Since PHE had a higher octanol–water partition coefficient ($\log K_{ow}$) compared with NAP (Table 1), a high affinity between PHE and WAC surface was confirmed. It has been reported that the pollutants with higher values of $\log K_{ow}$ would present a powerful trend of adsorption over AC.[38] Meanwhile, compared with PHE, NAP performed higher water solubility, lower molecular weight and octanol–water partition coefficient, indicating that NAP had relatively high polarity. Moreover, the surface of AC was considered to be non-polar which contributes to the adsorption of non-polar substances rather than polar substances, resulting in a lower adsorption of NAP. Moreover, the pore size distribution of WAC and the size of the contaminants were also crucial factors that affected the adsorption process.[21] The importance of adsorbing target compound from water through the microporous region of WAC had been discussed in the characterization and the batch adsorption experiment section.

### 3.6. Monte-Carlo simulations

With the aim to further prove the existence of the preferential adsorption behavior of WAC towards NAP and PHE, Monte-Carlo simulations were employed to explore the interaction of NAP or PHE on WAC using the Adsorption Locator code form the Materials Studio 7.0.[25,26] Many possible adsorption patterns of NAP or PHE molecule adsorbing on the surface of WAC were discovered (Fig. S1 and S2†). The optimized complexes of NAP- and PHE-WAC are depicted in Fig. S3,† respectively, where the PHE formed bonds of 2.392 Å, 2.622 Å, or 5.432 Å with the atoms on the surface of WAC, and another PHE molecule was combined with WAC at a suitable distance. The adsorption energy ($E_{ad}$)[38] was calculated as $E_{ad} = E_{adsorbate} + E_{cluster} - E_{system}$, and the results are listed in Table 6. Consequently, PHE-WAC performed a higher calculated value of $E_{ad}$ (83.881 a.u.) than that of NAP-WAC (41.859 a.u), indicating that the combination of PHE-WAC was stronger than NAP-WAC and therefore exhibited a higher preferential adsorption.[39] Thus, the results of the preferential adsorption obtained from the experiment (PHE > NAP) was convincing.

### 3.7. Adsorption mechanisms

To investigate the necessity of diffusion and mass transfer steps in the adsorption process, intraparticle diffusion and film diffusion models were performed,[35] which can be expressed as:

$$\text{Intraparticle diffusion model: } Q_t = K_{id} t^{0.5} + C \quad (17)$$

$$\text{Film diffusion model: } -\ln(1 - Q_t/Q_e) = K_{fd} t \quad (18)$$

Where, $K_{id}$ and $K_{fd}$ (mg g$^{-1}$ min$^{-0.5}$) are the intraparticle diffusion and liquid film diffusion rate constants, respectively; and $C$ is the intercept related to the boundary layer effect.

Fig. 9 illustrates the fitting of the kinetic data over different diffusion models, the corresponding parameters and $R^2$ are all summarized in Table 7. As shown in Fig. 9a, two different steps of diffusion were observed. The first step of a higher slope ($K_{id1}$) for all condition, representing external diffusion of PAHs on the WAC surface; the second step shows a decrease in the slope ($K_{id2}$) because of the increasing rate of adsorption reflected that the adsorption stage where intraparticle diffusion; however, the

Table 6 The adsorption energy ($E_{ad}$) of NAP-WAC and PHE-WAC from adsorption locator

| $E_{ad}$ | WAC-1 | WAC-2 | WAC-3 | WAC-4 | WAC-5 | WAC-6 | WAC-7 | WAC-8 | WAC-9 | WAC-10 |
|---|---|---|---|---|---|---|---|---|---|---|
| NAP-WAC | 41.854 | 41.856 | 41.859 | 41.846 | 41.845 | 41.844 | 41.843 | 41.841 | 41.840 | 41.840 |
| PHE-WAC | 83.847 | 83.854 | 83.849 | 83.881 | 83.845 | 83.844 | 83.843 | 83.838 | 83.834 | 83.829 |

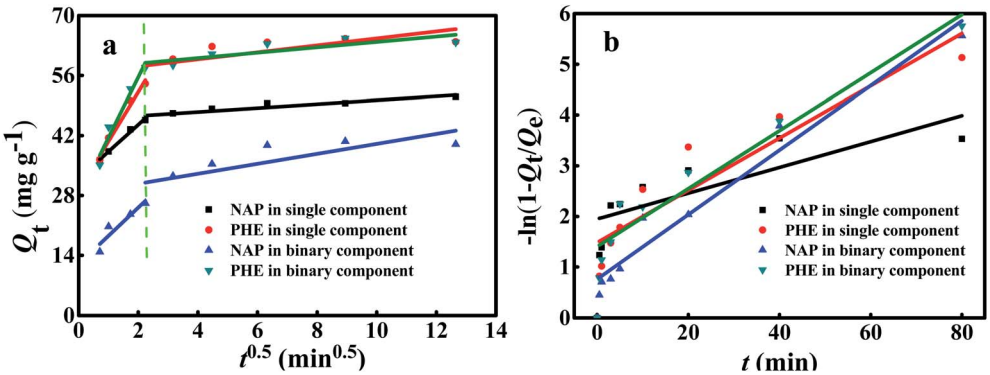


Fig. 9 Intraparticle diffusion (a) and film diffusion models (b) for the single and binary component systems.

Table 7 Intraparticle diffusion and film diffusion parameters for single- and binary-component systems

| | | Intraparticle diffusion model | | | | Film diffusion model | |
|---|---|---|---|---|---|---|---|
| | | Step 1 | | Step 2 | | | |
| Systems | | $K_{id1}$ | $R^2$ | $K_{id2}$ | $R^2$ | $K_{fd}$ | $R^2$ |
| Single solute | NAP | 6.28 | 0.985 | 0.458 | 0.825 | 0.025 | 0.857 |
| | PHE | 11.50 | 0.975 | 0.816 | 0.498 | 0.052 | 0.866 |
| Binary solute | NAP | 6.63 | 0.826 | 1.165 | 0.565 | 0.064 | 0.964 |
| | PHE | 14.33 | 0.932 | 0.629 | 0.652 | 0.057 | 0.942 |

third region did not exist due to adsorption has been reached the equilibrium state.[28] In addition, the linear curves did not pass through the origin demonstrated that intraparticle diffusion was involved in the adsorption process. Nevertheless, it was not the foremost step of the mechanism.[9] Thus, the film diffusion model was applied to further analyze the kinetic data. The relevant results are presented in Fig. 9b and Table 7. The $R^2$ of intraparticle diffusion model were smaller than those of the film diffusion model. This finding demonstrated that film diffusion mainly controlled the adsorption of PAHs onto WAC. Similar solute-surface diffusion mechanisms for PAHs adsorption onto ammonia-modified CAC had also been reported.[40]

## 4. Conclusions

In this study, we prepared a WNS-based microporous activated carbon (WAC) with high total pore volume and specific surface area under microwave-assisted conditions for the adsorption of NAP and PHE from aqueous solution. The characterization of WAC exhibited that it has abundant surface functional groups and developed pore structure. The preferential adsorption of PHE over WAC was determined in the binary-component system during the batch adsorption process. The kinetic data were fitted better to pseudo-second-order model and the WAC exhibits high adsorption capacity for NAP and PHE at low pH. Due to the non-polar interaction between the uncharged molecules of PAHs and WAC surface, the maximum adsorption capacity of NAP and PHE were 93.62 and 145.62 mg g$^{-1}$ at pH 3, respectively. Equilibrium data was favorably described by Freundlich isotherm in single system, and competitive adsorption was evaluated by SRS model in binary component systems. Theoretical calculations shows that the values of separation factor for PHE-NAP were greater than unity in all case, and Monte-Carlo simulations demonstrates that PHE-WAC had a higher calculated value of $E_{ad}$ than that of NAP-WAC, these results demonstrate the preferential adsorption of PHE from different perspectives. Furthermore, the adsorption of PAHs onto WAC was mainly governed by film diffusion mass transfer mechanism. We believe that microwave-assisted is a promising method for the preparation of a green adsorbents, and our work can contribute to the research progress of competitive adsorption and purification of PAHs from water environment.

## Conflicts of interest

There are no conflicts to declare.

## Acknowledgements

This work was supported financially by funding from the National Natural Science Foundation of China (21868034) and the International Science and Technology Cooperation Program of Shihezi University (GJHZ201601).

## References

1 P. Liu, Z. Wu, X. Ge and X. Yang, Hydrothermal synthesis and microwave-assisted activation of starch-derived carbons as an effective adsorbent for naphthalene removal, *RSC Adv.*, 2019, **9**, 11696–11706.
2 F. M. T. Luna, C. C. B. Araújo, C. B. Veloso, I. J. Silva, D. C. S. Azevedo and C. L. Cavalcante, Adsorption of naphthalene and pyrene from isooctane solutions on commercial activated carbons, *Adsorption*, 2011, **17**, 937–947.
3 F. M. T. Luna, A. N. Oliveira Filho, C. C. B. Araújo, D. C. S. Azevedo and C. L. Cavalcante, Adsorption of polycyclic aromatic hydrocarbons from heavy naphthenic oil using commercial activated carbons. 2. Column

 

adsorption studies, *Ind. Eng. Chem. Res.*, 2016, **55**, 8184–8190.

4 M. Zhu, J. Yao, L. Dong and J. Sun, Adsorption of naphthalene from aqueous solution onto fatty acid modified walnut shells, *Chemosphere*, 2016, **144**, 1639–1645.

5 H. S. Niasar, H. Li, T. V. R. Kasanneni, M. B. Ray and C. Xu, Surface amination of activated carbon and petroleum coke for the removal of naphthenic acids and treatment of oil sands process-affected water (OSPW), *Chem. Eng. J.*, 2016, **293**, 189–199.

6 A. S. Bausk and B. I. Dvorak, Selecting the column configuration with lowest media replacement cost for small adsorption systems, *Water Res.*, 2016, **93**, 38–47.

7 Z. Wu, X. Wei, Y. Xue, X. He and X. Yang, Removal effect of atrazine in co-solution with Bisphenol A or humic acid by different activated carbons, *Materials*, 2018, **11**, 1–13.

8 R. R. Pawar, Lalhmunsiama, H. C. Bajaj and S.-M. Lee, Activated bentonite as a low-cost adsorbent for the removal of Cu(II) and Pb(II) from aqueous solutions: Batch and column studies, *J. Ind. Eng. Chem.*, 2016, **34**, 213–223.

9 A. Benhouria, M. A. Islam, H. Zaghouane-Boudiaf, M. Boutahala and B. H. Hameed, Calcium alginate–bentonite–activated carbon composite beads as highly effective adsorbent for methylene blue, *Chem. Eng. J.*, 2015, **270**, 621–630.

10 K. Y. Foo and B. H. Hameed, Mesoporous activated carbon from wood sawdust by $K_2CO_3$ activation using microwave heating, *Bioresour. Technol.*, 2012, **111**, 425–432.

11 M. A. Islam, I. A. W. Tan, A. Benhouria, M. Asif and B. H. Hameed, Mesoporous and adsorptive properties of palm date seed activated carbon prepared via sequential hydrothermal carbonization and sodium hydroxide activation, *Chem. Eng. J.*, 2015, **270**, 187–195.

12 B. Cabal, T. Budinova, C. O. Ania, B. Tsyntsarski, J. B. Parra and B. Petrova, Adsorption of naphthalene from aqueous solution on activated carbons obtained from bean pods, *J. Hazard. Mater.*, 2009, **161**, 1150–1156.

13 H. Gupta and B. Gupta, Adsorption of polycyclic aromatic hydrocarbons on banana peel activated carbon, *Desalin. Water Treat.*, 2015, **57**, 9498–9509.

14 D. Ding, Y. Zhao, S. Yang, W. Shi, Z. Zhang, Z. Lei and Y. Yang, Adsorption of cesium from aqueous solution using agricultural residue–Walnut shell: Equilibrium, kinetic and thermodynamic modeling studies, *Water Res.*, 2013, **47**, 2563–2571.

15 X. Zheng, H. Lin, Y. Tao and H. Zhang, Selective adsorption of phenanthrene dissolved in Tween 80 solution using activated carbon derived from walnut shells, *Chemosphere*, 2018, **208**, 951–959.

16 S. Teixeira, C. Delerue-Matos and L. Santos, Application of experimental design methodology to optimize antibiotics removal by walnut shell based activated carbon, *Sci. Total Environ.*, 2019, **646**, 168–176.

17 D. Liu, Z. Wu, X. Ge, G. Cravotto, Z. Wu and Y. Yan, Comparative study of naphthalene adsorption on activated carbon prepared by microwave-assisted synthesis from different typical coals in Xinjiang, *J. Taiwan Inst. Chem. Eng.*, 2016, **59**, 563–568.

18 X. Xiao, D. Liu, Y. Yan, Z. Wu, Z. Wu and G. Cravotto, Preparation of activated carbon from Xinjiang region coal by microwave activation and its application in naphthalene, phenanthrene, and pyrene adsorption, *J. Taiwan Inst. Chem. Eng.*, 2015, **53**, 160–167.

19 W. Ao, J. Fu, M. Xiao, Q. Kang, C. Ran, Y. Liu, H. Zhang, Z. Gao, J. Li, G. Liu and J. Dai, Microwave assisted preparation of activated carbon from biomass: a review, *Renewable Sustainable Energy Rev.*, 2018, **92**, 958–979.

20 S. Hamidouche, O. Bouras, F. Zermane, B. Cheknane, M. Houari, J. Debord, M. Harel, J.-C. Bollinger and M. Baudu, Simultaneous sorption of 4-nitrophenol and 2-nitrophenol on a hybrid geocomposite based on surfactant-modified pillared-clay and activated carbon, *Chem. Eng. J.*, 2015, **279**, 964–972.

21 C. K. Ahn, S. H. Woo and J. M. Park, Selective adsorption of phenanthrene in nonionic–anionic surfactant mixtures using activated carbon, *Chem. Eng. J.*, 2010, **158**, 115–119.

22 W. Zhou, X. Wang, C. Chen and L. Zhu, Removal of polycyclic aromatic hydrocarbons from surfactant solutions by selective sorption with organo-bentonite, *Chem. Eng. J.*, 2013, **233**, 251–257.

23 F. Zermane, O. Bouras, M. Baudu and J.-P. Basly, Cooperative coadsorption of 4-nitrophenol and basic yellow 28 dye onto an iron organo–inorgano pillared montmorillonite clay, *J. Colloid Interface Sci.*, 2010, **350**, 315–319.

24 K. Y. Ho, G. McKay and K. L. Yeung, Selective adsorbents from ordered mesoporous silica, *Langmuir*, 2003, **19**, 3019–3024.

25 D. Bahamon and L. F. Vega, Pharmaceuticals removal from water effluents by adsorption in activated carbons using Monte Carlo simulations, *Langmuir*, 2017, **33**, 11146–11155.

26 R. Diao, H. Zhang, D. Zhao and S. Li, Adsorption and structure of benzene, toluene, and p-xylene in carbon slit pores: A Monte Carlo simulation study, *Chem. Eng. Sci.*, 2019, **197**, 120–134.

27 J. Liang, X. Li, Z. Yu, G. Zeng, Y. Luo, L. Jiang, Z. Yang, Y. Qian and H. Wu, Amorphous $MnO_2$ modified biochar derived from aerobically composted swine manure for adsorption of Pb(II) and Cd(II), *ACS Sustainable Chem. Eng.*, 2017, **5**, 5049–5058.

28 K. C. Bedin, A. C. Martins, A. L. Cazetta, O. Pezoti and V. C. Almeida, KOH-activated carbon prepared from sucrose spherical carbon: Adsorption equilibrium, kinetic and thermodynamic studies for methylene blue removal, *Chem. Eng. J.*, 2016, **286**, 476–484.

29 Z. Yu, C. Zhang, Z. Zheng, L. Hu, X. Li, Z. Yang, C. Ma and G. Zeng, Enhancing phosphate adsorption capacity of SDS-based magnetite by surface modification of citric acid, *Appl. Surf. Sci.*, 2017, **403**, 413–425.

30 C. Zhang, Z. Yu, G. Zeng, B. Huang, H. Dong, J. Huang, Z. Yang, J. Wei, L. Hu and Q. Zhang, Phase transformation of crystalline iron oxides and their adsorption abilities for Pb and Cd, *Chem. Eng. J.*, 2016, **284**, 247–259.

31 K. Amstaetter, E. Eek and G. Cornelissen, Sorption of PAHs and PCBs to activated carbon: coal versus biomass-based quality, *Chemosphere*, 2012, **87**, 573–578.
32 E. M. Ö. Kaya, A. S. Özcan, Ö. Gök and A. Özcan, Adsorption kinetics and isotherm parameters of naphthalene onto natural- and chemically modified bentonite from aqueous solutions, *Adsorption*, 2013, **19**, 879–888.
33 X. Guo, L. Luo, Y. Ma and S. Zhang, Sorption of polycyclic aromatic hydrocarbons on particulate organic matters, *J. Hazard. Mater.*, 2010, **173**, 130–136.
34 X. Ge, Z. Wu, Z. Wu, Y. Yan, G. Cravotto and B.-C. Ye, Enhanced PAHs adsorption using iron-modified coal-based activated carbon via microwave radiation, *J. Taiwan Inst. Chem. Eng.*, 2016, **64**, 235–243.
35 M. Yuan, S. Tong, S. Zhao and C. Q. Jia, Adsorption of polycyclic aromatic hydrocarbons from water using petroleum coke-derived porous carbon, *J. Hazard. Mater.*, 2010, **181**, 1115–1120.
36 X. Tang, Y. Zhou, Y. Xu, Q. Zhao, X. Zhou and J. Lu, Sorption of polycyclic aromatic hydrocarbons from aqueous solution by hexadecyltrimethylammonium bromide modified fibric peat, *J. Chem. Technol. Biotechnol.*, 2010, **85**, 1084–1091.
37 S. Debnath, N. Ballav, A. Maity and K. Pillay, Competitive adsorption of ternary dye mixture using pine cone powder modified with β-cyclodextrin, *J. Mol. Liq.*, 2017, **225**, 679–688.
38 A. Kiejna and T. Pabisiak, Effect of substrate relaxation on adsorption energies: The example of $\alpha$-$Fe_2O_3(001)$ and $Fe_3O_4(111)$, *Surf. Sci.*, 2019, **679**, 225–229.
39 J. L. Sotelo, G. Ovejero, A. Rodríguez, S. Álvarez, J. Galán and J. García, Competitive adsorption studies of caffeine and diclofenac aqueous solutions by activated carbon, *Chem. Eng. J.*, 2014, **240**, 443–453.
40 X. Ge, Z. Wu, Z. Wu, Y. Yan, G. Cravotto and B.-C. Ye, Microwave-assisted modification of activated carbon with ammonia for efficient pyrene adsorption, *J. Ind. Eng. Chem.*, 2016, **39**, 27–36.

 